Water Practice & Technology

IWA PUBLISHING

Water Practice & Technology Vol 18 No 12, 3255 doi: 10.2166/wpt.2023.203

Application of oak charcoal-based activated carbon for the removal of methylene blue dye from aqueous solutions: kinetics, equilibrium, and reusability studies

Kosar Kouhi[a], Abdoliman Amouei[b], Hosseinali Asgharnia[b], Mehdi Vosoughi[c], Seyede Houriye Fallah[b] and Mohammad Shirmardi[b,d,*]

[a] Student Research Committee, Babol University of Medical Sciences, Babol, Iran
[b] Department of Environmental Health Engineering, School of Public Health, Babol University of Medical Sciences, Babol, Iran
[c] Department of Environmental Health Engineering, School of Public Health, Ardabil University of Medical Sciences, Ardabil, Iran
[d] Social Determinants of Health Research Center, Health Research Institute, Babol University of Medical Sciences, Babol, Iran
*Corresponding author. E-mail: shirmardim@yahoo.com

ABSTRACT

The present study investigated the use of oak charcoal-based activated carbon (OC-AC) as an adsorbent for the removal of methylene blue (MB) dye from aqueous solutions. The study examined the effects of key operational variables, including pH, equilibrium time, adsorbent dosage, and initial dye concentration. The results showed that pH had no significant effect on MB adsorption for the initial MB concentration below 50 mg L^{-1} and an adsorbent dosage of 1 g L^{-1}, but increasing the contact time and adsorbent dosage improved the removal efficiency. For instance, at an initial MB concentration of 50 mg L^{-1}, the removal percentage increased from 76 to 99.9%, with increasing adsorbent dosage from 0.5 to 3 g L^{-1}. In addition, with increasing contact time from 5 to 300 min, the removal percentage increased from 45.43 to 87.42%. The study also analyzed the kinetics and isotherm behavior of MB adsorption and found that the Avrami fractional order kinetic model and the Freundlich isotherm model provided the best fit for the experimental data. MB removal from real water samples showed that OC-AC could be used as an efficient and environmentally friendly adsorbent for removing MB dye from contaminated effluents with the removal percentage ranging from 83 to 97%.

Key words: activated carbon, adsorption, aqueous solutions, methylene blue

HIGHLIGHTS

- Activated carbon was prepared from oak charcoal as low-cost precursors.
- The effects of operational variables on the adsorption of methylene blue dye were investigated.
- The experimental data were fitted to nonlinear kinetic and isotherm models.
- The Avrami fractional order kinetic model and the Freundlich isotherm model well described the adsorption process.

GRAPHICAL ABSTRACT

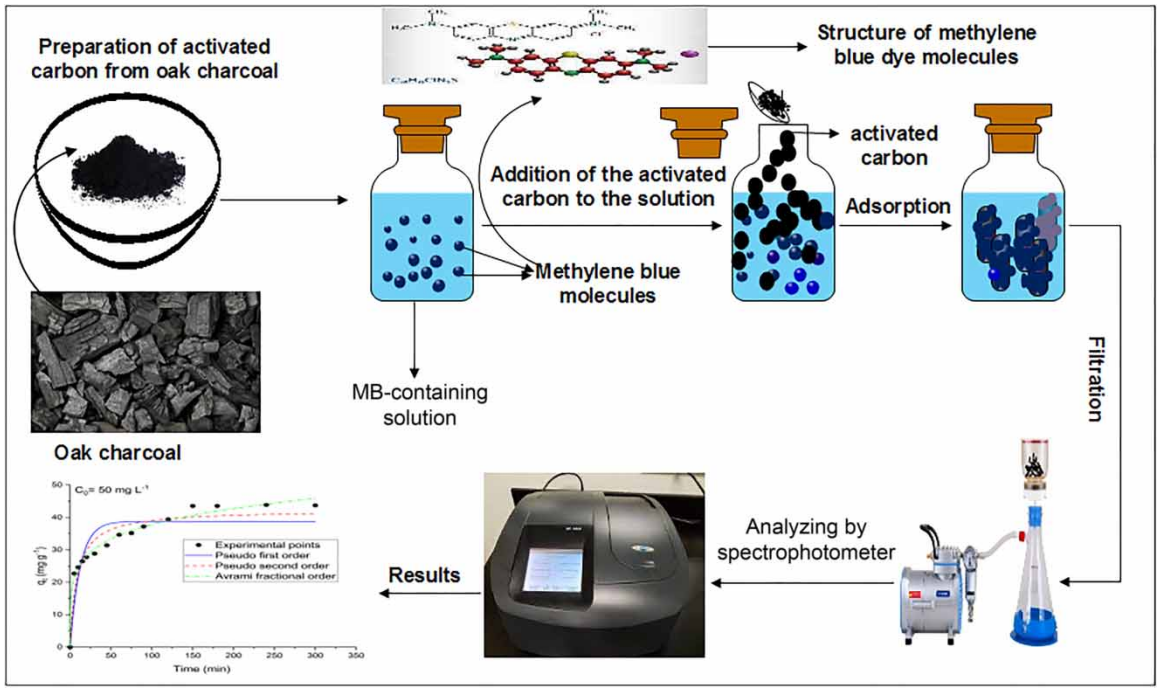

INTRODUCTION

The quality of many water bodies has deteriorated due to a variety of factors such as population growth, rapid and unplanned urbanization, industrialization, technological expansion, energy consumption, and waste generation from domestic and industrial sources. This deterioration has rendered many water bodies unwholesome and hazardous to the health of both humans and other living organisms. In developing countries, contaminated water is responsible for 80% of all diseases, as stated by the World Health Organization. Industrial effluents are often major contributors to a wide range of water pollution problems (Amuda & Ibrahim 2006; Sharifian *et al.* 2017).

Synthetic dyes and pigments are widely used in various industries worldwide, producing over 7×10^7 tons of dyestuff annually (Al-Tohamy *et al.* 2022). However, the discharge of colored wastewater carrying residual dyes from these industries poses significant environmental problems. The presence of even trace amounts of dyes in water is remarkably visible, objectionable, and undesirable and can negatively affect the public perception of water quality. Moreover, some synthetic dyes and their metabolites are highly toxic, potentially carcinogenic, mutagenic, and allergenic to the exposed organism (Rafatullah *et al.* 2010; Rehman *et al.* 2012; Chequer *et al.* 2013; Gholami-Borujeni *et al.* 2013; Zhou *et al.* 2014).

Methylene blue (MB) is a cationic dye commonly used in the colorization of cotton, silk, and wood. When dissolved in water, it produces a deep blue color. However, MB is harmful in nature and can cause allergies, irritation, vomiting, breathing difficulties, diarrhea, and nausea when ingested or inhaled (Ullah *et al.* 2022).

Based on current scientific knowledge, it is imperative to treat dye-contaminated effluents using appropriate methods prior to discharge into the receiving water bodies. Failure to do so can result in adverse impacts on aquatic life and the environment. Therefore, it is crucial to implement effective treatment strategies to mitigate the harmful effects of dye pollution on the ecosystem (Afshin *et al.* 2019; Dolas 2023).

Various treatment methods such as physical, biological, chemical oxidation (such as ozonation), advanced oxidation (such as photocatalytic decomposition), electrocoagulation, nanoparticles, ion exchange, and membrane separation processes are available to remove dyes from industrial effluents (Ullah *et al.* 2022; Dolas 2023). However, due to high cost and operational problems associated with these methods, their use is not cost-effective for many countries. For instance, the coagulation and filtration method produces a high amount of secondary waste. Dyes are also resistant to aerobic biodegradation and are not eliminated by conventional biological processes. Membrane processes are costly and require specialized personnel to operate.

The large-scale application of chemical oxidation methods is not feasible in the industry (Al-Tohamy *et al.* 2022).

Among the available options, the adsorption process is widely used due to its high efficiency, ease of operation, insensitivity to toxic compounds, and the availability of a wide range of adsorbents. The adsorption method produces a high-quality effluent that does not contain harmful substances such as ozone and free radicals (Shirmardi *et al.* 2016; Putranto *et al.* 2022; Ullah *et al.* 2022). Activated carbon (AC), sugarcane pulp ash, rice husk ash, coconut husk, magnesium chloride, and chitosan are some of the adsorbents tested for removing dyes. AC, in particular, is widely used due to its high adsorption capacity and regenerability. However, commercial ACs are generally expensive, and researchers are exploring the production of ACs using sustainable and cost-effective resources. One promising avenue is the use of agricultural resources, waste materials, and by-products to produce AC. AC derived from waste residues has received significant attention due to its renewability, low cost, and eco-friendliness (Gholami Borujeni *et al.* 2013; Xue *et al.* 2022; Bouchelkia *et al.* 2023). Numerous studies have been carried out by researchers to develop low-cost AC using various materials for the adsorption of dyes. For instance, Weng *et al.* (2009) used pineapple leaf powder as an adsorbent for the removal of MB dye from aqueous solutions. In addition, comprehensive lists and reviews are available that cover various types of adsorbents for the removal of dyes (Sharma *et al.* 2009; Weng *et al.* 2009; Pathania *et al.* 2017; Naushad *et al.* 2019; Nizam *et al.* 2021).

Despite the fact that many low-cost adsorbents have been studied for the removal of MB dye and decontamination purposes, studies on the application of oak charcoal-based AC (OC-AC) as a cheap and economical adsorbent for MB dye removal are limited. Therefore, this study aims to investigate the use of oak charcoal, a cheap, readily available, and natural adsorbent, for removing MB dye from aqueous solutions after preparation, activation, and surface functionalization. The study will also evaluate the effects of pH, contact time, adsorbent dose, initial dye concentration, and temperature on the efficiency of the adsorption process. The adsorption kinetic and equilibrium data were also fitted to the nonlinear form of the related models.

MATERIALS AND METHODS

Chemicals and reagents

All chemicals and reagents utilized in this study were of high analytical purity and were purchased from a reputable supplier. To adjust the pH value of the solutions, hydrochloric acid (HCl) and sodium hydroxide (NaOH) solutions were employed. MB, which is also known as tetramethylthionine chloride, was employed as the adsorbate in this study. MB is a cationic thiazine dye with a complex aromatic structure; its International Union of Pure and Applied Chemistry (IUPAC) name is 3,7-bis(dimethylamino)phenothiazin-5-ium chloride, and its chemical formula is $C_{16}H_{18}N_3SCl$. The MB dye used in this study was purchased from Merck Company. Its molecular weight, maximum adsorption wavelength, and water solubility are 319.85 g mol^{-1}, 665 nm, and 40 g L^{-1}, respectively. The chemical structure of MB dye is depicted in Figure 1.

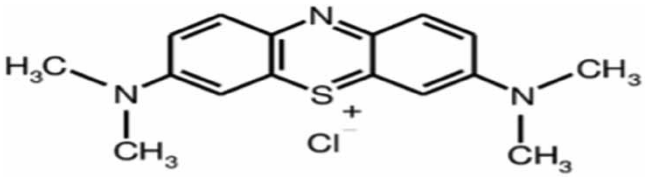

Figure 1 | Chemical structure of MB dye.

Preparation and characterization of the OC-AC adsorbent

The oak charcoals used in this study as the starting raw materials were prepared by the natives of Lordegan county, Chaharmahal and Bakhtiari province, Iran, who live in the foothills of the Zagros mountain range. The oak charcoals were produced by a traditional procedure. The purchased charcoals were washed several times with distilled water, were boiled in distilled water for 1 h to remove impurities and ashes, and then dried in an oven at 110 °C overnight.

The dried charcoals were ground and sieved to discrete smaller particles with the size of ≤300 μm. After separating the particles, a chemical method was used to prepare and activate the adsorbent. A mixture of $FeCl_3$, $ZnCl_2$, KOH, and lime (a weight ratio of 35:35:15:15) was used for the chemical activation. The prepared sample had an inorganic:organic weight ratio of 1:1. After adding the chemicals to the raw oak charcoals, 200 mL of distilled water was added to the resulting mixture to form a homogeneous composition and dissolve the chemicals. The mixture was refluxed at 100 °C under magnetic stirring conditions for 1 h, filtered, and then dried overnight at 100 °C. After drying, it was stored in a desiccator for the final activation step.

To complete the final activation of the pretreated charcoal, it was activated in a furnace under nitrogen atmosphere at the temperature range of 30–700 °C. The temperature was increased by 10 °C min^{-1}, and the rate of nitrogen gas flow was 150 mL min^{-1}. The mixture was kept at 700 °C for 1 h and then cooled under a nitrogen atmosphere. After cooling, the charcoal was washed with 6 M HCl to remove impurities and mineral residues. Finally, the activated charcoals were rinsed several times with distilled water to adjust the pH to a range of 6–7, dried overnight in an oven, and kept in an appropriate glass container for further applications (Shirmardi *et al.* 2016; Takdastan *et al.* 2016). The OC-AC adsorbent was characterized by several techniques, and the associated details are presented in the Supplementary Material.

Adsorption experiments

Batch adsorption experiments were carried out using laboratory bottles containing 50 mL of MB aqueous solution. The effects of the most important operational parameters including solution pH (range 3–11), contact time (5–300 min), adsorbent dosage (0.5–3 g L^{-1}), initial MB concentration (10–150 mg L^{-1}), and temperature (20–45 °C) were evaluated and optimized. All experiments were conducted on a magnetic stirrer or in an incubator shaker at a constant agitation speed of 250 rpm. To run an experiment, the other variables were kept constant at the predetermined value. Blank experiments were also run in parallel with no adsorbent added under the same conditions to determine if the pH of the MB solution affected MB adsorption and to examine the possibility of the adsorption of MB onto the bottles and to exclude the effects of other variables on the MB adsorption.

Kinetics study

The speed of the adsorption process, controlled by kinetics, is an important factor in designing an adsorption system. Kinetics determines the speed of the dye removal process and the effect of reaction time on the removal efficiency of a contaminant. Adsorption kinetics were used to determine the mechanism controlling the adsorption processes, either chemical reactions or diffusion mechanisms, which determine the factors affecting the reaction rate. To determine the kinetics of MB adsorption by OC-AC, nonlinear equations of the pseudo-first-order, pseudo-second-order, Avrami fractional order (AFO) kinetic models, and intra-particles diffusion model were employed to fit and describe the experimental data. Equations (1)–(4) present these kinetics models, respectively (Weber & Morris 1963; Lopes *et al.* 2003; Ho 2006; Liu & Liu 2008; Liu & Shen 2008; Cardoso *et al.* 2011; Alencar *et al.* 2012):

$$q_t = q_e \cdot [1 - \exp(-k_f \cdot t)] \tag{1}$$

$$q_t = \frac{k_s \times q_e^2 \times t}{1 + q_e \times k_s \times t} \tag{2}$$

$$q_t = q_e \cdot [1 - \exp(-k_{AV} \cdot t)^{n_{AV}}] \tag{3}$$

$$q_t = k_{id}\sqrt{t} + C \tag{4}$$

where t, q_t, and q_e represent the contact time (min), the amount of adsorbate (MB dye in this study) adsorbed at time t (mg g^{-1}), and the amount of adsorbate (MB) adsorbed at the equilibrium (mg g^{-1}), respectively. k_f, k_s, and k_{AV} are the pseudo-first-order rate constant (min^{-1}), the pseudo-second-order rate constant (g mg^{-1} min^{-1}), and the Avrami kinetic constant (min^{-1}), respectively; n_{AV} is a fractional adsorption order, which is related to the adsorption mechanism. The parameters k_{id} (mg g^{-1} $min^{-0.5}$) and C (mg g^{-1}) refer to the adsorption rate constant of the intraparticle diffusion model and the intercept of the stage related to the thickness of the boundary layer, respectively. By plotting q_t vs. $t^{0.5}$, k_{id} and C can be directly obtained from the slope and intercept of the plot (Lima *et al.* 2015; Putranto *et al.* 2022).

Equilibrium studies

The study aimed to determine the homogeneous and heterogeneous characteristics of adsorption isotherm models. To evaluate the adsorption isotherms, the nonlinear equations of the Langmuir (Langmuir 1918), the Freundlich (Freundlich 1906), and the Liu (Liu *et al.* 2003) models, as shown in Equations (5)–(7), were used to describe and fit the experimental adsorption data:

$$q_e = \frac{Q_{max} \times K_L \times C_e}{1 + K_L \times C_e} \tag{5}$$

$$q_e = K_F \times C_e^{1/n_F} \tag{6}$$

$$q_e = \frac{Q_{max} \times (K_g \times C_e)^{n_L}}{1 + (K_g \times C_e)^{n_L}} \tag{7}$$

where q_e, C_e, and Q_{max} represent the amount of adsorbate (MB) adsorbed at the equilibrium (mg g^{-1}), the concentration of the adsorbate (mg L^{-1}) at the equilibrium condition, and the maximum adsorption capacity of the adsorbent (mg g^{-1}), respectively. K_L, K_F, and K_g are the Langmuir equilibrium constant (L mg^{-1}), Freundlich equilibrium constant [mg g^{-1} (mg L^{-1})$_F^{-1/n}$], and Liu equilibrium constant (L mg^{-1}), respectively; n_F and n_L are the dimensionless exponents of Freundlich and Liu models, respectively.

Determination of final concentration of MB

The final concentration of MB in the aqueous solution was determined using a UV–Vis spectrophotometer (DR5000, Hach Company, USA) at a wavelength of 665 nm. First, a calibration curve was prepared using a series of standard solutions of known MB concentrations. The absorbance of each standard solution was measured at 665 nm, and a calibration curve was plotted using the absorbance values and corresponding concentrations. The concentration of MB in the aqueous solution was then determined by measuring its absorbance and interpolating its concentration from the calibration curve. The measurement was repeated three times for each sample, and the mean value was used for further analysis. The accuracy of the spectrophotometric measurements was verified by comparing the measured values with the known concentrations of the standard solutions. The percent recovery of the standard solutions was found to be within the acceptable range of 95–105%. After each run, the sample was immediately filtered using a 0.22-μm membrane filter to remove adsorbent particles from the solution.

The removal percentage of MB, the amount of MB adsorbed at time t (q_t, mg g^{-1}), and the amount of MB adsorbed at equilibrium (q_e, mg g^{-1}) was calculated using Equations (8)–(10), respectively:

$$\text{MB removal } \% = \frac{(C_0 - C_e)}{C_0} \times 100 \tag{8}$$

$$q_t = \frac{(C_0 - C_t) \times V}{M} \tag{9}$$

$$q_e = \frac{(C_0 - C_e) \times V}{M} \tag{10}$$

where C_0 and C_e are the initial and equilibrium concentrations of MB in the solution, respectively (mg L^{-1}); M (g), V (L), C_t (mg L^{-1}), and q_t (mg g^{-1}) are the mass of the adsorbent, the volume of the solution, the concentration of MB at time t, and the amount of MB adsorbed onto the adsorbent at time t, respectively.

Statistical evaluation of kinetic and isotherm parameters

This study utilized a nonlinear approach to fit both the kinetic and equilibrium data. Specifically, the Levenberg–Marquardt algorithm was utilized for calculating successive interactions. In addition, interactions were computed via the Simplex method through the nonlinear fitting capabilities of OriginPro software. The suitability of the evaluated models was compared based on a determination coefficient (R^2), an adjusted determination coefficient (R^2_{adj}), and a standard deviation (SD). The SD represents the variation between the theoretical value of q that the model predicts and the q that is measured experimentally. The corresponding mathematical expressions for R^2,

R^2_{adj}, and SD are presented in Equations (11)–(13), respectively:

$$R^2 = \left(\frac{\sum_i^n (q_{i,\exp} - \bar{q}_{\exp})^2 - \sum_i^n (q_{i,\exp} - q_{i,model})^2}{\sum_i^n (q_{i,\exp} - \bar{q}_{\exp})^2} \right) \tag{11}$$

$$R^2_{adj} = 1 - (1 - R^2) \times \left(\frac{n-1}{n-p-1} \right) \tag{12}$$

$$SD = \sqrt{\left(\frac{1}{n-p} \right) \times \sum_i^n (q_{i,\exp} - q_{i,model})^2} \tag{13}$$

In these equations, $q_{i,\exp}$ is the value of q obtained from experimental measurements, while $q_{i,model}$ is the predicted value of q derived from the model. The average value of all q obtained through experimental measurements is represented by $\bar{q}_{\exp}$; n denotes the total number of experiments conducted, and p refers to the number of parameters in the fitted model (dos Santos *et al.* 2015; Saucier *et al.* 2015c).

Regeneration and reusability of the adsorbent

Following the adsorption process, the OC-AC adsorbent was dispersed in a solution of HCl (0.1 mol L^{-1}) and agitated for 1 h to regenerate and reuse the exhausted adsorbent. After the desired time, the adsorbent was separated from the solution by decanting process and rinsed with deionized water to remove any residual acid and dye completely. Finally, OC-AC was placed inside an oven at 100 °C overnight. The regeneration procedure was repeated for five cycles. The efficiency of the regenerated adsorbent was assessed through adsorption experiments, measuring the dye removal efficiency and comparing it to the initial performance of the adsorbent (Buelvas *et al.* 2023).

RESULTS AND DISCUSSION

Characterization of the OC-AC adsorbent

To determine some characteristics of the OC-AC adsorbent, such as the phases on the adsorbent structure, surface morphology, elemental composition (chemical composition), functional groups on the adsorbent surface, and specific surface area, X-ray diffraction (XRD), field emission scanning electron microscopy, energy-dispersive X-ray spectrometry, Fourier transform infrared, and Brunauer–Emmett–Teller (BET) analyses were carried out to characterize the OC-AC adsorbent.

The XRD pattern of the prepared AC is shown in Fig. 1S. The XRD pattern of the AC shows a wide peak at 2θ between 13 and 35°. This broad peak can be related to amorphous carbon (Saucier *et al.* 2015a). In addition, four peaks associated with other crystalline phases left in the XRD pattern of the AC even after leaching with 6 M HCl (Saucier *et al.* 2015b). These peaks can be indexed to calcium carbide (CaC_2: JCPDS card 01-075-1558) and calcium chloride carbide ($Ca_3Cl_2C_3$: JCPDS card 076-0298). For more details about the characterization of OC-AC, please see the Supplementary Material.

Effect of pH

The presence and abundance of anionic and/or cationic ions in the surrounding environment can influence the interactions between the adsorbent and the target molecule or ion for adsorption. Therefore, the adsorption process is significantly influenced by the pH of the adsorbate solution, as it can affect the chemistry of both the adsorbent and the adsorbate.

In this study, the effects of solution pH on the removal of MB dye using OC-AC were investigated at different pH values for dye concentrations of 50 and 100 mg L^{-1} and adsorbent dosage of 1 and 2 g L^{-1}. The other experimental conditions were kept constant. Figure 2 illustrates the effect of pH on MB adsorption from aqueous solutions onto OC-AC. For the initial dye concentration of 100 mg L^{-1} and an adsorbent dosage of 1 g L^{-1}, as the pH value of the solution increased from 3 to 11, the adsorption of MB onto OC-AC increased from 71 to 87%. For other initial dye concentrations and adsorbent dosages, the adsorption efficiency of MB dye onto OC-AC increased gradually with an increase in pH until it reached its maximum value. However, the increase was not significant for adsorbent dosage of 2 g L^{-1} and initial dye concentration less than 100 mg L^{-1} because

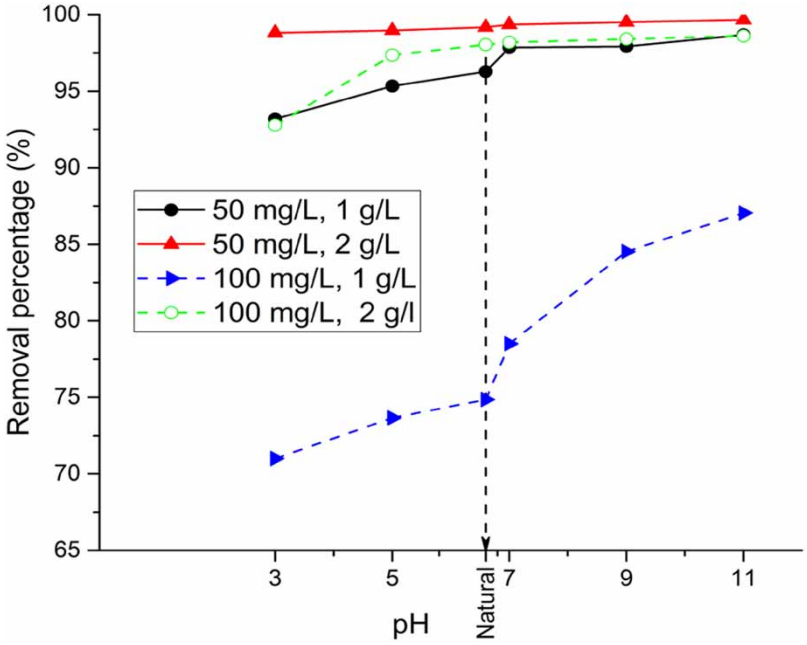

Figure 2 | Effect of pH on the adsorption of MB onto the OC-AC adsorbent (experimental conditions – MB concentration: 50 and 100 mg L^{-1}, room temperature, adsorbent quantity: 1 and 2 g L^{-1}, and contact time: 2 h).

all dye molecules were relatively removed from the solutions, indicating the high efficiency of OC-AC toward MB dye at a wide pH range. The consistent removal percentage observed across the studied pH range may be attributed to the abundance of adsorption sites compared to the number of MB molecules, despite any changes in pH that could alter the ratio of positive and negative charges on the adsorbent surface. In an acidic medium (pH < 5), excess H^+ ions that are present for the protonation of the active sites of the adsorbent compete with MB cationic species to adsorb onto the surface of OC-AC, resulting in a reduced adsorption efficiency. On the other hand, the increased adsorption of MB in the basic range is attributed to an increase in hydroxyl ions on the surface of OC-AC, which provides a negative charge to OC-AC. These hydroxide ions increase the attraction force between the negatively charged surface of OC-AC and MB cationic molecules ($pk_a = 3.8$) (De Castro *et al.* 2018; Farooq *et al.* 2022; Bouchelkia *et al.* 2023; Dolas 2023). Another possible mechanism could involve the formation of hydrogen bonds between the active sites of the adsorbent and the MB molecules. The hydrogen portion of the OH group in the OC-AC structure may be attracted to the lone pairs of electrons on the nitrogen species of the MB aromatic rings, resulting in the formation of hydrogen bonds and the subsequent adsorption of MB molecules (Said *et al.* 2023).

The results of current research are in line with the findings of other similar studies (De Castro *et al.* 2018; Ivanets *et al.* 2022). To avoid the inclusion of extra ions resulting from pH adjustment using acids or alkalis, further adsorption tests were conducted under the original or natural pH conditions.

Kinetics experiments

Adsorption kinetics is an important phenomenon that describes the rate at which adsorbate molecules are taken up by the adsorbent material over time (Farooq *et al.* 2022). The selection of an appropriate kinetic model is crucial for accurate analysis and understanding of the adsorption behavior of a target pollutant (dos Reis *et al.* 2023). In this study, we investigated the kinetic behavior of MB dye adsorption onto the OC-AC adsorbent using the pseudo-first-order, pseudo-second-order, AFO, and intraparticle diffusion kinetic models.

The experiment was carried out by adding OC-AC to a series of solutions with two different initial concentrations of 25 and 50 mg L^{-1} of MB dye. The solutions were then agitated for varying time intervals ranging from 5 to 300 min. The results of the experiment showed that the adsorption of MB dye onto OC-AC was fast at the initial stages and then became slower as time progressed (Figure 3). The experimental results revealed that, for an initial concentration of 25 mg L^{-1}, 59% of the total removal (99.9%) occurred during the first 10 min of contact time. However, for a higher MB concentration of 50 mg L^{-1}, only 50% of the total removal

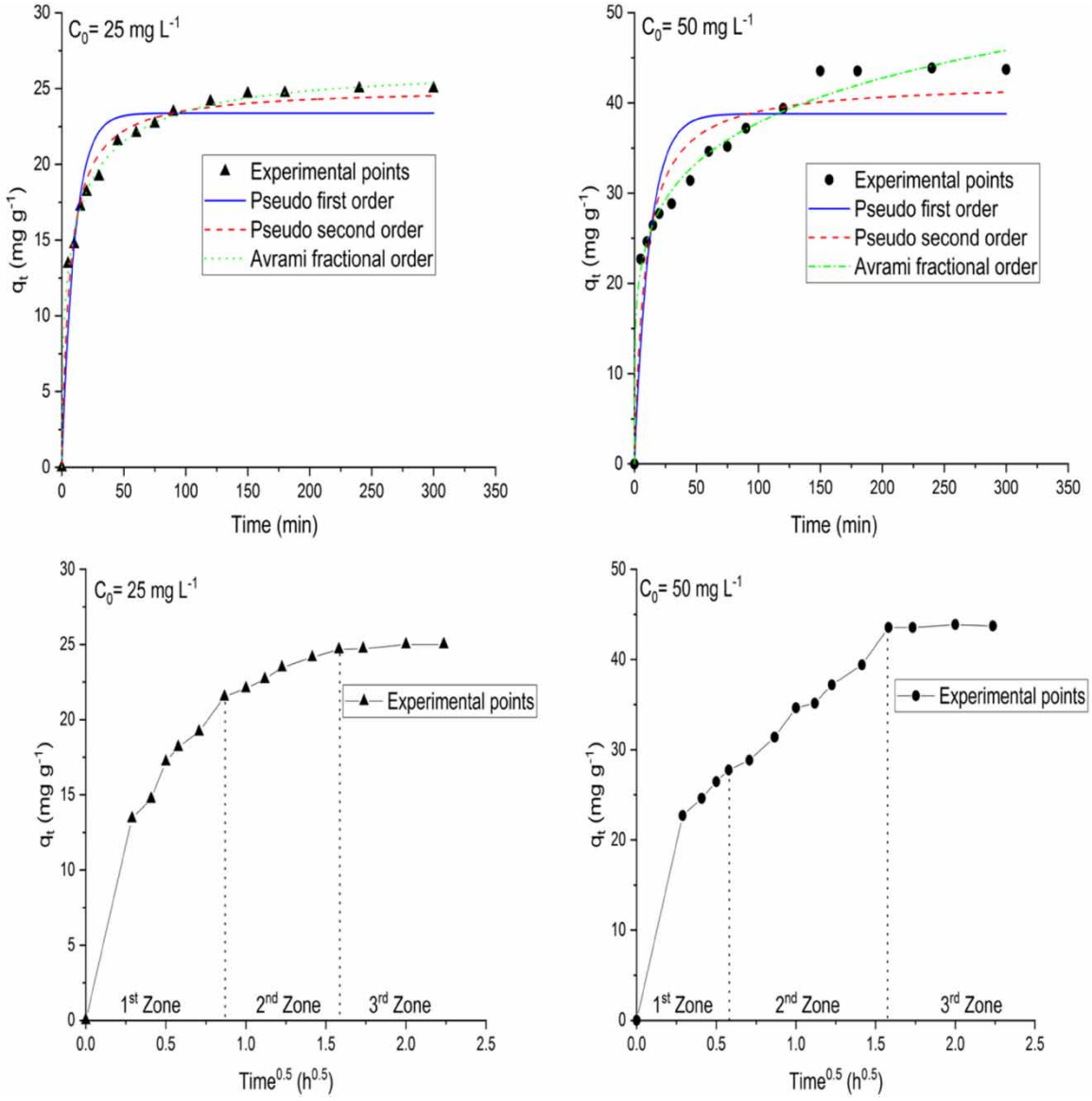

Figure 3 | Kinetic models for the adsorption of MB dye at room temperature (experimental conditions – adsorbent quantity: 1 g L^{-1}; MB concentration: 25 and 50 mg L^{-1}, and natural pH of solutions).

(96%) was achieved during the same period. The adsorption process reached equilibrium at approximately 120 min for both concentrations. This behavior is characteristic of adsorption kinetics, where the concentration of the adsorbate reduces over time, leading to saturation of the adsorbent surface with adsorbed molecules (dos Reis *et al.* 2023).

The adsorption capacity (q_t) increased from 23 to 44 mg g^{-1} with increasing time from 5 to 300 min (for MB concentration of 50 mg L^{-1}), indicating that OC-AC was effective in removing the dye from the solutions. In our study, we evaluated the goodness of fit of the nonlinear kinetic models to the experimental data by analyzing the adjusted R^2 and the SD values. The SD values indicate the degree of deviation between the theoretically calculated q value and the experimentally measured q value. A higher SD value suggests a greater degree of discrepancy between the two values (dos Reis *et al.* 2023).

In this study, SD values were calculated for the three different kinetic models. The SD ratio was then used to compare the fitness of each individual model. As presented in Table 1, for an MB concentration of 25 mg L^{-1}, SD values for the pseudo-first-order, pseudo-second-order, and AFO kinetic models were 1.88, 0.93, and 0.38, respectively. The corresponding values for the MB concentration of 50 mg L^{-1} were 5.02, 3.35, and 1.35, respectively. In addition, for the MB concentration of 25 mg L^{-1}, the SD ratio values for the pseudo-first-

Table 1 | Parameters of the fitted models for MB dye adsorption

	Initial MB concentration (mg L^{-1})	
Kinetic parameter	**25**	**50**
Pseudo-first-order		
q_e (mg g^{-1})	23.38	38.8
k_f (min^{-1})	0.098	0.082
R^2_{adj}	0.93	0.83
SD (mg g^{-1})	1.88	5.02
Pseudo-second-order		
q_e (mg g^{-1})	25.05	42.36
K_s (g mg^{-1} min^{-1})	0.0063	0.0028
R^2_{adj}	0.982	0.9221
SD (mg g^{-1})	0.93	3.35
AFO		
q_e (mg g^{-1})	26	122
k_{AV} (min^{-1})	0.0783	1.058×10^{-4}
n_{AV}	0.414	0.218
R^2_{adj}	0.9973	0.9883
SD (mg g^{-1})	0.38	1.35
Intraparticle diffusion model		
K_{id} (mg g^{-1} $h^{-0.5}$)[a]	4.56	15.47
R^2_{adj}	0.98	0.9485

[a]Second zone.

order, pseudo-second-order, and AFO kinetic models were found to be 4.95, 2.45, and 1, respectively (Table 1). For the MB concentration of 50 mg L^{-1}, the corresponding values were 3.72, 2.48, and 1, respectively. Based on Figure 3, it is obvious that for both MB concentrations, the AFO kinetic model provided the best fit to the experimental data, as evidenced by the lowest SD ratio values and the highest adjusted coefficient of determination (R^2_{adj}) values (Table 1). The AFO model proposes that the adsorption is a complex process with numerous potential pathways. Changes in the adsorption mechanism occur during the process, and the kinetics may follow multiple orders that vary over time as the adsorbent and adsorbate interact. Typically, the n_{AV} exponent takes on a fractional value, in agreement with the predictions of the AFO model (Cimirro *et al.* 2022; dos Reis *et al.* 2023).

To further investigate the effect of mass transfer resistance on the adsorption process, we applied the intraparticle diffusion model. The plots of the amount adsorbed (q_t) vs. the square root of time ($t^{0.5}$) showed multilinearity, indicating that the adsorption process involved more than one adsorption rate (dos Reis *et al.* 2023; Singh *et al.* 2023). Each linear section was ascribed to a particular stage of the adsorption process. The first linear section corresponded to the external surface adsorption, which involved the diffusion of MB molecules from the bulk solution to the external surface of the OC-AC adsorbent. The second linear section was attributed to the intraparticle diffusion, which involved the diffusion of MB molecules from the external surface to the interior pores of the OC-AC adsorbent. The third linear section corresponded to the diffusion through smaller pores (dos Reis *et al.* 2023; Singh *et al.* 2023).

The results of the kinetic studies revealed that the minimum contact time required to reach equilibrium for the adsorption of MB onto the OC-AC adsorbent was about 120 min. To ensure that equilibrium was attained even at higher concentrations, we fixed the contact time at 180 min for the rest of our experimental work.

Effect of adsorbent dosage

Adsorbent dosage is a crucial factor that affects the efficiency of the adsorption process. The amount of adsorbent added to the system has a direct impact on the removal efficiency of the adsorbent and optimization of the

process. Increasing the adsorbent dosage provides more surface area for adsorption, resulting in higher contact between the adsorbate and the adsorbent (Wu *et al.* 2022). In the present study, the adsorbent dosage was varied from 0.5 to 3 g L^{-1}, and its effect on the removal percentage and adsorption capacity (q_e) of the adsorbent was investigated for two initial MB concentrations of 50 and 100 mg L^{-1}.

The results showed that increasing the adsorbent dosage from 0.5 to 3 g L^{-1} for an initial MB concentration of 50 mg L^{-1} led to an increase in the removal percentage from 76 to 99.9% (no dye was visually observed). This is because increasing the adsorbent dose increases the number of active sites available for adsorption, resulting in higher removal efficiency. However, the removal percentage becomes constant at a certain point, indicating that further increase in the adsorbent dose does not significantly affect the removal percentage (Shirmardi *et al.* 2016; Wu *et al.* 2022). In addition, increasing the adsorbent dose resulted in a decrease in the adsorption capacity (q_e) from 76 to 17 mg g^{-1}. This is due to a decrease in the number of active sites per unit mass of adsorbent (Shirmardi *et al.* 2016; Wu *et al.* 2022). The corresponding changes for the initial MB concentration of 100 mg L^{-1} were 69–99.9% for removal efficiency and 138–33 mg g^{-1} for adsorption capacity (q_e). Figure 4 provides a clear visual representation of the effect of adsorbent dosage on the removal percentage and adsorption capacity of the adsorbent. The results highlight the importance of optimizing the adsorbent dosage to achieve maximum removal efficiency and adsorption capacity.

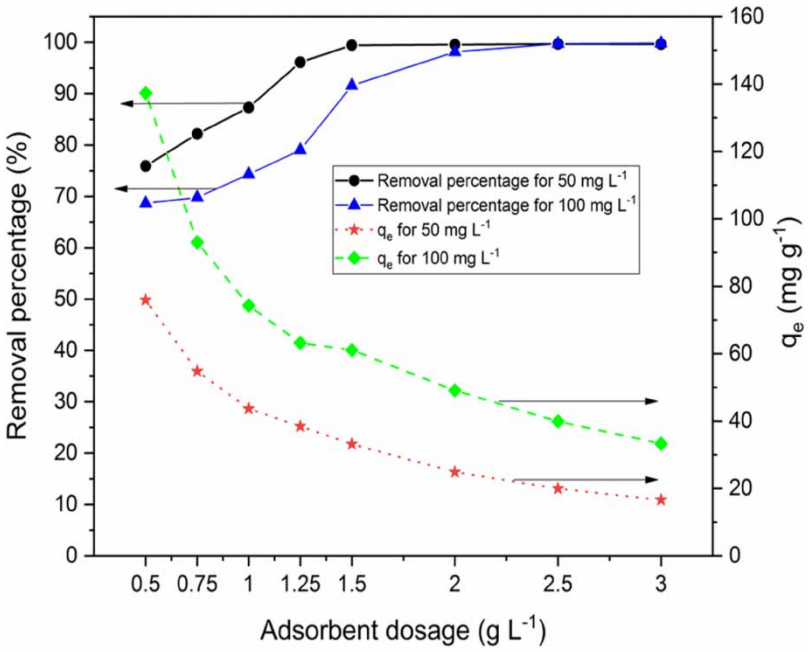

Figure 4 | Effect of adsorbent dosage on the adsorption of MB dye (experimental conditions – natural pH; room temperature; contact time: 180 min, and initial MB concentration: 50 and 100 mg L^{-1}).

Effect of initial MB concentration, temperature, and equilibrium studies

In this study, the adsorption of MB dye onto the OC-AC adsorbent was evaluated using nonlinear equations of three popular adsorption isotherm models: Langmuir, Freundlich, and Liu. The experimental data were collected at different MB concentrations (ranging from 10 to 150 mg L^{-1}) and temperatures (room temperatures of 20–22, 35, and 45 °C) under previously optimized experimental conditions. Our results revealed that the removal percentage of MB decreased as the initial concentration of MB increased. For example, at room temperature, the removal percentage decreased from 100 to 75% as the initial dye increased from 10 to 150 mg L^{-1}. This decrease is due to the fact that as the initial concentration of MB increases, the amount of available adsorption sites on the adsorbent decreases because of the increased number of dye molecules in the solution.

Moreover, our findings showed that the amount of MB adsorbed (q_e) onto the surface of OC-AC increased with increasing the temperature from 20 to 35 °C. This could be attributed to the increased mobility of MB molecules at a higher temperature of 35 °C, which enhances the interaction between the dye molecules and the solid adsorbent. However, at 45 °C, compared to 35 °C, the removal percentage and q_e were not changed significantly and slightly decreased for higher concentrations (90–150 mg L^{-1}), indicating that there may be a limit to the reduction of MB concentration at high temperatures. We compared the goodness of fit of the models based on the SD values and adjusted R^2. Our results indicated that the Langmuir model did not accurately describe the equilibrium data as it showed the highest SD and the lowest adjusted R^2 values compared to the other models studied. Conversely, the Freundlich and Liu models provided a good fit for the equilibrium data. However, the Freundlich model exhibited the lowest SD values, indicating that it provided the best fit to the experimental data across all studied temperatures.

The data associated with the effects of initial MB concentration, temperature, and adsorption isotherms of MB dye are presented in Figure 5(a)–5(c), while Table 2 shows the parameters predicted by the models.

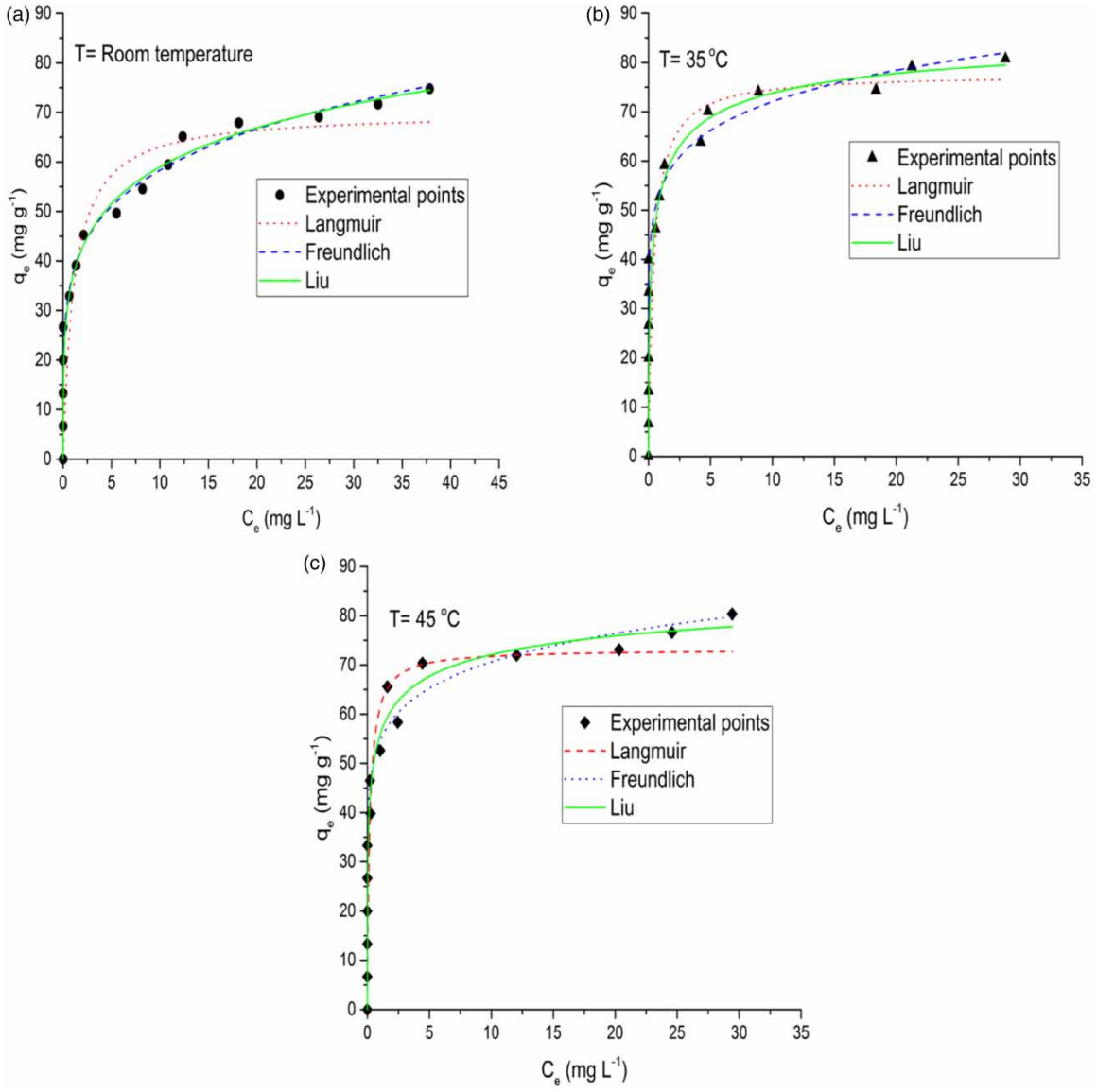

Figure 5 | Isotherm models for the adsorption of MB dye using the OC-AC adsorbent at different temperatures: (a) room temperature of 20–22 °C, (b) 35 °C, and (c) 45 °C (experimental conditions – adsorbent dosage: 1.5 g L^{-1}; contact time: 180 min, and natural pH of solution).

Table 2 | Isotherm parameters for the adsorption of MB dye using the OC-AC adsorbent

Temperature (°C)	Room temperature	35	45
Langmuir			
Q_{max} (mg g^{-1})	70.05	77.65	73.2
K_L (L mg^{-1})	0.9	2.37	5.06
R^2_{adj}	0.81	0.6	0.73
SD	10.7	17.16	14.07
Freundlich			
K_f (mg g^{-1} (mg L^{-1})$^{-1/nf}$)	37.43	54.42	54.38
n_f	5.2	8.2	8.82
R^2_{adj}	0.84	0.6	074
SD	9.92	17.14	13.67
Liu			
Q_{max} (mg g^{-1})	179.2	89.64	92.83
K_g (L mg^{-1})	0.0079	2.3	2.96
n_L	0.28	0.49	0.37
R^2_{adj}	0.83	0.57	0.73
SD	10.28	17.72	14.08

Conditions: adsorbent quantity 1.5 g L^{-1}, contact time 180 min, and natural pH of solutions.

Reusability of the adsorbent

AC is a widely used adsorbent for the removal of various pollutants from aqueous solutions, and its efficacy is largely determined by its reusability or recyclability. In this regard, the potential of OC-AC as a reusable adsorbent for the removal of MB dye was investigated over five consecutive cycles in the present study. The results showed that OC-AC could effectively remove the MB dye from aqueous solutions with a removal efficiency of up to 99.9%. Interestingly, the OC-AC adsorbent demonstrated excellent reusability over five consecutive cycles with a slight decrease in removal efficiency after each cycle. The removal efficiency of OC-AC decreased from 99.9% in the first cycle to 90.2% in the fifth cycle, indicating that the adsorbent can be used repeatedly without a significant decline in its adsorption capacity (Figure 6). The ability to reuse the adsorbent multiple times not only reduces the cost of the adsorption process but also has a positive environmental impact by reducing the amount of waste generated from the adsorbent.

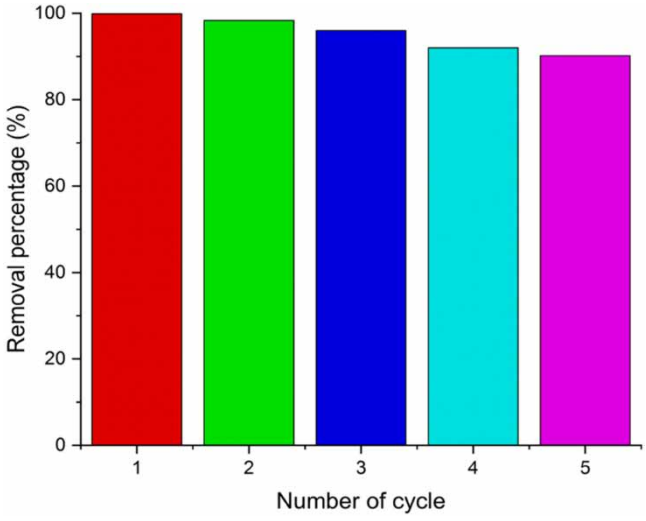

Figure 6 | Desorption and reusability study for the adsorption of MB dye onto the OC-AC adsorbent.

Adsorption of MB dye from real water samples

It is essential to assess the effectiveness of adsorbents in a multipollutant environment that mimics real wastewater effluents, rather than synthetic ones. Therefore, water samples were collected from the Caspian Sea and Babolrood river (Mazandaran province, Iran) to investigate the efficiency of the OC-AC adsorbent for the removal of MB dye and to evaluate the possible effects of competitive ions on MB removal percentage. Some physicochemical characteristics of the water samples are presented in Table 1S. Three different concentrations of MB (25, 50, and 100 mg L^{-1}) were spiked into the water samples and treated with the OC-AC adsorbent at natural pH of water samples. Distilled water was used as a control sample. When using an adsorbent dosage of 1 g L^{-1}, the removal percentage for the seawater samples was in the range of 83–94% and for river water samples was in the range of 84–94.5%. The corresponding removal percentage for the blank samples ranged from 85 to 99%. The experimental results shown in Figure 7 demonstrate that OC-AC can be used as an adsorbent to efficiently remove MB from real samples without significant changes in its removal efficiency.

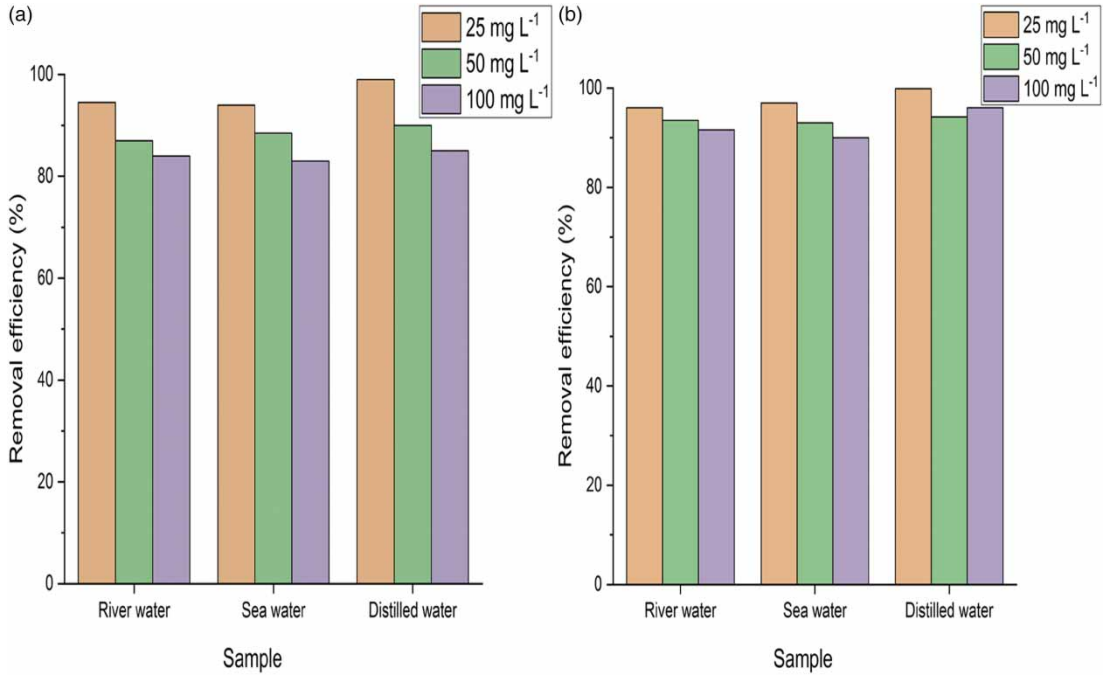

Figure 7 | Removal of MB dye from real water samples: (a) adsorbent dosage: 1 g L^{-1} and (b) adsorbent dosage: 1.5 g L^{-1} (experimental conditions – contact time 180 min and natural pH of solutions).

CONCLUSION

The present study investigated the potential of OC-AC as an adsorbent for the removal of MB dye from aqueous solutions. The results showed that OC-AC was effective in removing MB, with a high removal percentage achieved under optimized conditions. The adsorption kinetics and isotherm behavior of OC-AC were also analyzed, and the AFO kinetic model and the Freundlich isotherm model provided the best fit to the experimental data. In addition, the OC-AC adsorbent was found to be reusable for up to five cycles without significant loss of its removal percentage (range: 90.2–99.9%). Therefore, OC-AC can be considered a low-cost environmentally friendly adsorbent for the removal of MB dye from contaminated effluents with a removal percentage in the range of 90–97% when using an adsorbent dosage of 1.5 g L^{-1}. This study provides useful information for researchers and practitioners in the field of water and wastewater treatment, particularly in the textile and dyeing industries.

ACKNOWLEDGEMENTS

This research is approved and supported by Student Research Committee, Babol University of Medical Sciences (IRCT code: IR.MUBABOL.HRI.REC.1401.029). The authors sincerely thank the Vice-Chancellor for Research

and Technology of Babol University of Medical Sciences for the financial support. The authors also acknowledge the School of Public Health for providing necessary facilities to accomplish this research.

DATA AVAILABILITY STATEMENT

All relevant data are included in the paper or its Supplementary Information.

CONFLICT OF INTEREST

The authors declare there is no conflict.

REFERENCES

Afshin, S., Rashtbari, Y., Shirmardi, M., Vosoughi, M. & Hamzehzadeh, A. 2019 Adsorption of basic violet 16 dye from aqueous solution onto mucilaginous seeds of *Salvia sclarea*: Kinetics and isotherms studies. *Desalination and Water Treatment* **161**, 365–375.

Alencar, W. S., Lima, E. C., Royer, B., dos Santos, B. D., Calvete, T., da Silva, E. A. & Alves, C. N. 2012 Application of aqai stalks as biosorbents for the removal of the dye Procion Blue MX-R from aqueous solution. *Separation Science and Technology* **47**(3), 513–526. doi:10.1080/01496395.2011.616568.

Al-Tohamy, R., Ali, S. S., Li, F., Okasha, K. M., Mahmoud, Y. A. G., Elsamahy, T., Jiao, H., Fu, Y. & Sun, J. 2022 A critical review on the treatment of dye-containing wastewater: Ecotoxicological and health concerns of textile dyes and possible remediation approaches for environmental safety. *Ecotoxicology and Environmental Safety* **231**, 113160. https://doi.org/10.1016/j.ecoenv.2021.113160.

Amuda, O. & Ibrahim, A. 2006 Industrial wastewater treatment using natural material as adsorbent. *African Journal of Biotechnology* **5**(16), 1483–1487.

Bouchelkia, N., Tahraoui, H., Amrane, A., Belkacemi, H., Bollinger, J.-C., Bouzaza, A., Zoukel, A., Zhang, J. & Mouni, L. 2023 Jujube stones based highly efficient activated carbon for methylene blue adsorption: Kinetics and isotherms modeling, thermodynamics and mechanism study, optimization via response surface methodology and machine learning approaches. *Process Safety and Environmental Protection* **170**, 513–535. https://doi.org/10.1016/j.psep.2022.12.028.

Buelvas, D. D. A., Camargo, L. P., Salgado, I. K. I., Vicentin, B. L. S., Valezi, D. F., Dall'Antonia, L. H., Tarley, C. R. T. & Mauro, E. D. 2023 Study and optimization of the adsorption process of methylene blue dye in reusable polyaniline-magnetite composites. *Synthetic Metals* **292**, 117232. https://doi.org/10.1016/j.synthmet.2022.117232.

Cardoso, N. F., Lima, E. C., Pinto, I. S., Amavisca, C. V., Royer, B., Pinto, R. B., Alencar, W. S. & Pereira, S. F. P. 2011 Application of cupuassu shell as biosorbent for the removal of textile dyes from aqueous solution. *Journal of Environmental Management* **92**(4), 1237–1247. http://dx.doi.org/10.1016/j.jenvman.2010.12.010.

Chequer, F. D., De Oliveira, G. R., Ferraz, E. A., Cardoso, J. C., Zanoni, M. B. & De Oliveira, D. P. 2013 Textile dyes: Dyeing process and environmental impact. *Eco-friendly Textile Dyeing and Finishing* **6**(6), 151–176.

Cimirro, N. F. G. M., Lima, E. C., Cunha, M. R., Thue, P. S., Grimm, A., dos Reis, G. S., Rabiee, N., Saeb, M. R., Keivanimehr, F. & Habibzadeh, S. 2022 Removal of diphenols using pine biochar. Kinetics, equilibrium, thermodynamics, and mechanism of uptake. *Journal of Molecular Liquids* **364**, 119979. https://doi.org/10.1016/j.molliq.2022.119979.

De Castro, M. L. F. A., Abad, M. L. B., Sumalinog, D. A. G., Abarca, R. R. M., Paoprasert, P. & de Luna, M. D. G. 2018 Adsorption of methylene blue dye and Cu(II) ions on EDTA-modified bentonite: Isotherm, kinetic and thermodynamic studies. *Sustainable Environment Research* **28**(5), 197–205. https://doi.org/10.1016/j.serj.2018.04.001.

Dolas, H. 2023 Activated carbon synthesis and methylene blue adsorption from pepper stem using microwave assisted impregnation method: Isotherm and kinetics. *Journal of King Saud University – Science* **35**(3), 102559. doi:10.1016/j.jksus.2023.102559.

dos Reis, G. S., Bergna, D., Grimm, A., Lima, E. C., Hu, T., Naushad, M. & Lassi, U. 2023 Preparation of highly porous nitrogen-doped biochar derived from birch tree wastes with superior dye removal performance. *Colloids and Surfaces A: Physicochemical and Engineering Aspects* **669**, 131493. https://doi.org/10.1016/j.colsurfa.2023.131493.

dos Santos, D. C., Adebayo, M. A., Lima, E. C., Pereira, S. F., Cataluña, R., Saucier, C., Thueb, P. S. & Machadoe, F. M. 2015 Application of carbon composite adsorbents prepared from coffee waste and clay for the removal of reactive dyes from aqueous solutions. *Journal of the Brazilian Chemical Society* **26**(5), 924–938. http://dx.doi.org/10.5935/0103-5053.20150053.

Farooq, S., Al Maani, A. H., Naureen, Z., Hussain, J., Siddiqa, A. & Al Harrasi, A. 2022 Synthesis and characterization of copper oxide-loaded activated carbon nanocomposite: Adsorption of methylene blue, kinetic, isotherm, and thermodynamic study. *Journal of Water Process Engineering* **47**, 102692. doi:10.1016/j.jwpe.2022.102692.

Freundlich, H. 1906 Adsorption in solution. *Physical Chemistry Sociology* **40**, 1361–1368.

Gholami-Borujeni, F., Naddafi, K. & Nejatzade-Barandozi, F. 2013 Application of catalytic ozonation in treatment of dye from aquatic solutions. *Desalination and Water Treatment* **51**(34–36), 6545–6551. doi:10.1080/19443994.2013.769491.

Gholami Borujeni, F., Mahvi, A. H. & Nejatzadeh-Barandoozi, F. 2013 Removal of heavy metal ions from aqueous solution by application of low cost materials. *Fresenius Environmental Bulletin* **22**(3), 655–658.

Ho, Y.-S. 2006 Review of second-order models for adsorption systems. *Journal of Hazardous Materials* **136**(3), 681–689. http://dx.doi.org/10.1016/j.jhazmat.2005.12.043.

Ivanets, A., Prozorovich, V., Roshchina, M., Sychova, O., Srivastava, V. & Sillanpää, M. 2022 Methylene blue adsorption on magnesium ferrite: Optimization study, kinetics and reusability. *Materials Today Communications* **31**, 103594. https://doi.org/10.1016/j.mtcomm.2022.103594.

Langmuir, I. 1918 The adsorption of gases on plane surfaces of glass, mica and platinum. *Journal of the American Chemical Society* **40**(9), 1361–1403. doi:10.1021/ja02242a004.

Lima, É. C., Adebayo, M. A., Machado, F. M., 2015 Kinetic and equilibrium models of adsorption. In: *Carbon Nanomaterials as Adsorbents for Environmental and Biological Applications*, 1 edn. (Bergmann, C. P. & Machado, F. M., eds). Springer International Publishing, Switzerland, pp. 33–69.

Liu, Y. & Liu, Y.-J. 2008 Biosorption isotherms, kinetics and thermodynamics. *Separation and Purification Technology* **61**(3), 229–242. doi:10.1016/j.seppur.2007.10.002.

Liu, Y. & Shen, L. 2008 A general rate law equation for biosorption. *Biochemical Engineering Journal* **38**(3), 390–394. doi:10.1016/j.bej.2007.08.003.

Liu, Y., Xu, H., Yang, S.-F. & Tay, J.-H. 2003 A general model for biosorption of Cd^{2+}, Cu^{2+} and Zn^{2+} by aerobic granules. *Journal of Biotechnology* **102**(3), 233–239. http://dx.doi.org/10.1016/S0168-1656(03)00030-0.

Lopes, E. C. N., dos Anjos, F. S. C., Vieira, E. F. S. & Cestari, A. R. 2003 An alternative Avrami equation to evaluate kinetic parameters of the interaction of Hg(II) with thin chitosan membranes. *Journal of Colloid and Interface Science* **263**(2), 542–547. doi:10.1016/s0021-9797(03)00326-6.

Naushad, M., Alqadami, A. A., AlOthman, Z. A., Alsohaimi, I. H., Algamdi, M. S. & Aldawsari, A. M. 2019 Adsorption kinetics, isotherm and reusability studies for the removal of cationic dye from aqueous medium using arginine modified activated carbon. *Journal of Molecular Liquids* **293**, 111442. https://doi.org/10.1016/j.molliq.2019.111442.

Nizam, N. U. M., Hanafiah, M. M., Mahmoudi, E., Halim, A. A. & Mohammad, A. W. 2021 The removal of anionic and cationic dyes from an aqueous solution using biomass-based activated carbon. *Scientific Reports* **11**(1), 8623. doi:10.1038/s41598-021-88084-z.

Pathania, D., Sharma, S. & Singh, P. 2017 Removal of methylene blue by adsorption onto activated carbon developed from *Ficus carica* bast. *Arabian Journal of Chemistry* **10**, S1445–S1551. https://doi.org/10.1016/j.arabjc.2013.04.021.

Putranto, A., Ng, Z. W., Hadibarata, T., Aziz, M., Yeo, J. Y. J., Ismadji, S. & Sunarso, J. 2022 Effects of pyrolysis temperature and impregnation ratio on adsorption kinetics and isotherm of methylene blue on corn cobs activated carbons. *South African Journal of Chemical Engineering* **42**, 91–97. doi:10.1016/j.sajce.2022.07.008.

Rafatullah, M., Sulaiman, O., Hashim, R. & Ahmad, A. 2010 Adsorption of methylene blue on low-cost adsorbents: A review. *Journal of Hazardous Materials* **177**(1), 70–80. https://doi.org/10.1016/j.jhazmat.2009.12.047.

Rehman, M. S. U., Kim, I. & Han, J.-I. 2012 Adsorption of methylene blue dye from aqueous solution by sugar extracted spent rice biomass. *Carbohydrate Polymers* **90**(3), 1314–1322. https://doi.org/10.1016/j.carbpol.2012.06.078.

Said, H. A., Ait Bourhim, I., Ouarga, A., Iraola-Arregui, I., Lahcini, M., Barroug, A., Noukrati, H. & Ben youcef, H. 2023 Sustainable phosphorylated microcrystalline cellulose toward enhanced removal performance of methylene blue. *International Journal of Biological Macromolecules* **225**, 1107–1118. https://doi.org/10.1016/j.ijbiomac.2022.11.172.

Saucier, C., Adebayo, M. A., Lima, E. C., Cataluna, R., Thue, P. S., Prola, L. D., Puchana-Rosero, M. J., Machado, F. M., Pavan, F. A. & Dotto, G. L. 2015a Microwave-assisted activated carbon from cocoa shell as adsorbent for removal of sodium diclofenac and nimesulide from aqueous effluents. *Journal of Hazardous Materials* **289**, 18–27. doi:10.1016/j.jhazmat.2015.02.026.

Saucier, C., Adebayo, M. A., Lima, E. C., Cataluña, R., Thue, P. S., Prola, L. D. T., Puchana-Rosero, M. J., Machado, F. M., Pavan, F. A. & Dotto, G. L. 2015b Microwave-assisted activated carbon from cocoa shell as adsorbent for removal of sodium diclofenac and nimesulide from aqueous effluents. *Journal of Hazardous Materials* **289**, 18–27. https://doi.org/10.1016/j.jhazmat.2015.02.026.

Saucier, C., Adebayo, M. A., Lima, E. C., Prola, L. D. T., Thue, P. S., Umpierres, C. S., Rosero, M. J. P. & Machado, F. M. 2015c Comparison of a homemade bacuri shell activated carbon with carbon nanotubes for food dye removal. *CLEAN-Soil, Air, Water* **43**, 1389–1400. doi:10.1002/clen.201400669.

Sharifian, F., Shahidi, A. & Khashei, A. 2017 The survey of chromium (VI) adsorption from aqueous solutions by powder and activated carbon of pine cones. *Journal of Research in Environmental Health* **3**(3), 227–234.

Sharma, Y. C., Uma & Upadhyay, S. N. 2009 Removal of a cationic dye from wastewaters by adsorption on activated carbon developed from coconut coir. *Energy & Fuels* **23**(6), 2983–2988. doi:10.1021/ef9001132.

Shirmardi, M., Alavi, N., Lima, E. C., Takdastan, A., Mahvi, A. H. & Babaei, A. A. 2016 Removal of atrazine as an organic micro-pollutant from aqueous solutions: A comparative study. *Process Safety and Environmental Protection* **103**, 23–35. https://doi.org/10.1016/j.psep.2016.06.014.

Singh, S., Yadawa, Y. & Ranjan, A. 2023 Enhanced adsorption of methylene blue by mixed-phase bismuth ferrite prepared by non-aqueous sol-gel route. *Journal of Environmental Chemical Engineering* **11**(1), 109229. https://doi.org/10.1016/j.jece.2022.109229.

Takdastan, A., Mahvi, A. H., Lima, E. C., Shirmardi, M., Babaei, A. A., Goudarzi, G., Neisi, A., Farsani, M. H. & Vosoughi, M. 2016 Preparation, characterization, and application of activated carbon from low-cost material for the adsorption of tetracycline antibiotic from aqueous solutions. *Water Science and Technology* **74**(10), 2349–2363.

Ullah, N., Ali, Z., Ullah, S., Khan, A. S., Adalat, B., Nasrullah, A., Alsaadi, M. & Ahmad, Z. 2022 Synthesis of activated carbon-surfactant modified montmorillonite clay-alginate composite membrane for methylene blue adsorption. *Chemosphere* **309**(Pt 1), 136623. doi:10.1016/j.chemosphere.2022.136623.

Weber, W. J. & Morris, J. C. 1963 Kinetics of adsorption on carbon from solution. *Journal of the Sanitary Engineering Division* **89**(2), 31–60.

Weng, C.-H., Lin, Y.-T. & Tzeng, T.-W. 2009 Removal of methylene blue from aqueous solution by adsorption onto pineapple leaf powder. *Journal of Hazardous Materials* **170**(1), 417–424. https://doi.org/10.1016/j.jhazmat.2009.04.080.

Wu, T., Yang, G., Cao, J., Xu, Z. & Jiang, X. 2022 Activation and adsorption mechanisms of methylene blue removal by porous biochar adsorbent derived from eggshell membrane. *Chemical Engineering Research and Design* **188**, 330–341. https://doi.org/10.1016/j.cherd.2022.08.042.

Xue, H., Wang, X., Xu, Q., Dhaouadi, F., Sellaoui, L., Seliem, M. K., Ben Lamine, A., Belmabrouk, H., Bajahzar, A., Bonilla-Petriciolet, A., Li, Z. & Li, Q. 2022 Adsorption of methylene blue from aqueous solution on activated carbons and composite prepared from an agricultural waste biomass: A comparative study by experimental and advanced modeling analysis. *Chemical Engineering Journal* **430**, 132801. https://doi.org/10.1016/j.cej.2021.132801.

Zhou, C., Wu, Q., Lei, T. & Negulescu, I. I. 2014 Adsorption kinetic and equilibrium studies for methylene blue dye by partially hydrolyzed polyacrylamide/cellulose nanocrystal nanocomposite hydrogels. *Chemical Engineering Journal* **251**, 17–24. https://doi.org/10.1016/j.cej.2014.04.034.

First received 8 August 2023; accepted in revised form 30 October 2023. Available online 17 November 2023